Building a nucleic acid nanostructure with DNA-epitope conjugates for a versatile electrochemical protein detection platform

Asanka Gurukandure, Subramaniam Somasundaram, Amanda S. N. Kurian, Niamat Khuda, and Christopher J. Easley*

Department of Chemistry and Biochemistry, Auburn University, Auburn, AL 36849, USA

ABSTRACT: The recent surge of effort in nucleic acid-based electrochemical (EC) sensors has been fruitful, and some have even shown real-time quantification of drugs in the blood of living animals. Yet there remains a need for more generalizable EC platforms for the detection of multiple classes of clinically relevant targets. Our group has recently reported a nucleic acid nanostructure that permits simple, economical, and generalizable EC readout of a wide range of analytes (small molecules, peptides, large proteins, or antibodies). The DNA nanostructure is built through on-electrode enzymatic ligation of three oligonucleotides for attachment, binding, and signaling. However, the signaling mechanism predominantly relies on tethered diffusion of methylene blue at the electrode surface, limiting the detection of larger proteins that have no readily available small molecule binding partners. In this study, we adapted the nanostructure sensor to quantify larger proteins in a more generic manner, through conjugating the protein's minimized antibody-binding epitope to the central DNA strand of the nanostructure (DNA-peptide conjugate). This concept was verified using creatine kinase (CK-MM), an important biomarker of muscle damage, myocardial infarction, overexertion/rhabdomyolysis, or neuromuscular disorders where clinical outcomes could be improved with rapid sensing. DNA-epitope conjugates permitted a competitive immunoassay protocol at the electrode surface for quantifying CK protein. Square-wave voltammetry (SWV) signal suppression was proportional to the amount of surface-bound antibody with a limit of detection (LOD) of 5 nM and a response time as low as 3 minutes, and displacement of antibody by native CK-MM protein analyte could also be assayed. CK was quantified from the LOD of 14 nM up to 100 nM, overlapping well with the normal (non-elevated) human clinical range of 3 – 37 nM, and the sensor response was validated in 98% human serum. While a need for improved DNA-epitope conjugate purification was identified, overall this approach not only allows the detection of a generic protein- or peptide-binding antibody, but it also should facilitate future quantitative EC readout of various clinically relevant protein analytes that were previously inaccessible to EC techniques.

INTRODUCTION

Generalizable, point-of-care (POC) detection methods for clinically relevant proteins would greatly enhance healthcare management and disease diagnosis. Since POC methods tend to be cost-effective and user-friendly, they support at-home testing by patients[1, 2]. As the current benchmark technique, enzyme-linked immunosorbent assay (ELISA) has been used for detecting numerous clinically relevant analytes, and in some cases even single-molecule detection is achieved with high precision[3]. However, the needs for multiple washing steps, highly trained personnel, and expensive instruments has prompted the development of alternative, cost-effective, simpler methods[2, 4]. One more streamlined assay, AlphaLISA, is a bead-based luminescent amplification approach to quantify analytes in complex biofluids[5, 6]. Although it provides a better dynamic range, lower limit of detection, and easier workflow, the requirement of having expensive instrumentation limits its widespread usage. As such, researchers continue to seek strategies such as minimization of workflow and device miniaturization[7]. Microfluidics, electrochemistry, colorimetry, and temperature probes have all been proposed to achieve this goal[8-11]. Covid-19 test kits and pregnancy test kits are well-known POC devices based on lateral flow immunoassays. These kits can be obtained over-the-counter, which reduces laborious laboratory testing and assay time, but they provide qualitative rather than quantitative results[12]. Although POC methods are meant to operate in a limited resource setting, a key feature is that the assay should be sensitive and should provide accurate results regardless of the environment.

Electrochemical (EC) biosensors aid in overcoming these issues by providing assays which are quantitative, high sensitivity, and low cost while also being functional in human body fluids directly and capable of miniaturization for POC detection[11]. For example, continuous or near-continuous EC measurements for glucose, lactate, and neurotransmitters (dopamine, serotonin, glutamate, etc.) are available with customized enzymatic biosensors. However, this approach cannot easily be extended to detect other targets due to target-specific redox chemistry or its ability to

be oxidized by a specific enzyme [1, 2, 13-15]. Aptamer-based (E-AB) or nucleic acid/peptide-based EC biosensors have been investigated more recently to quantify clinically relevant analytes in biofluids in a fast, reagentless manner, sometimes even in whole blood or living animals [11, 16-18]. Although E-AB sensors provide promising results, finding a suitable aptamer for a wide range of targets is challenging, due to its requirement of being structure switching and complex selection process, making it harder to generalize[19]. Other electrochemical assay techniques such as DNA-based steric hindrance and nanoscale DNA molecular pendulum assays are capable of monitoring targets within several minutes in complex fluids and do not require structure switching molecules to recognize targets, showing their potential applicability as more generalizable POC method.[2, 17, 18, 20]

Shortened, antibody-binding epitopes have long been utilized for diagnosis with sensors, treatment, vaccine design, and disease prevention [21]. Improvements in biotechnology and bioinformatic tools have made it easier to map and synthesize such epitopes. Instead of employing the full antigen, a synthetic portion (epitope) can be used to trigger specific reactions, detect biomolecules, and produce vaccines. For biosensing of proteins, specifically, antibody-binding epitopes can be used in sensors to avoid using the large, native protein molecule, which can be conformationally sensitive or even unstable.[22] In one example, to quantify antibodies with a simple smartphone-based workflow, Merkx and coworkers developed a chemiluminescent proximity-based sensor through clever placement of two peptide epitopes.[7] Both the Kelley[23] and Lai [24] groups have used bioconjugates of peptide epitopes to detect HIV antibodies using EC. The Rant[25, 26] and Plaxco[27] groups have also made EC sensors of proteins by leveraging epitopes or protein domains attached to DNA-based sensors with copper-dependent nitrilotriacetic acid (NTA) binding to histidine tags on the peptides or proteins. These strategies have the potential to greatly expand the list of analytes accessible to EC sensors.

Recently our group introduced a novel architecture, the DNA nanostructure sensor, for more versatile detection of analytes.[28, 29] Similar to other methods, this approach leverages DNA-analyte conjugates[2, 17, 18] within the sensor architecture. Distinguishing features of our approach include being highly modular and providing consistent signal response with a variety of targets.[28, 29] Using the same core DNA nanostructure architecture, our sensors have been validated in 98% human serum for a variety of targets: small molecule drugs (tacrolimus) and biotechnology controls (biotin, digoxigenin), a peptide drug (exendin-4), and larger antibodies (anti-digoxigenin, anti-tacrolimus, anti-exendin). Thus, the sensor has been validated for generalizability for multiple analyte classes, all detectable in the nanomolar range. However, more generalized protein sensing has not yet been accomplished with this architecture. Because our signaling mechanism depends on the rate of tethered diffusion[30] of the labeled nanostructure, attaching a larger protein to the DNA structure will reduce the current significantly, and antibody addition will have little to no effect on the current—regardless of whether the protein analyte binds or not.

In this work, we show that by using a smaller DNA-peptide (i.e. DNA-epitope) conjugate as the recognition oligonucleotide in our nanostructure, a larger protein can be quantified through antibody displacement from the surface. We show that by conjugating the nanostructure with the minimized antibody-binding epitope of a protein, a significant level of tethered diffusion of our sensor is maintained, allowing quantification of subsequent antibody binding. In turn, this antibody binding can be used to sense the presence of the larger protein analyte. This novel protein sensor was verified using creatine kinase (CK), a biomarker of muscle damage, myocardial infarction, overexertion/rhabdomyolysis, and neuromuscular disorders. Similar to our recent work[28, 29], we then used antibody displacement for a fast, indirect, EC immunoassay of CK protein which was functional in 98% human serum within the clinical range of concentrations. This approach not only extended the generalizability of the DNA nanostructure sensor—likely to any generic protein with a known antibody—but it also provided a method to quantify a protein in the nanomolar range which was thus far not measured with direct EC methods.

EXPERIMENTAL

Reagents and Materials

All solutions were prepared with deionized, ultra-filtered water (Fisher Scientific). The following reagents were used as received. Magnesium chloride hexahydrate, tris-(2-carboxyethyl) phosphine hydrochloride (TCEP), 6-mercapto-hexanol (MCH), gold etchant, and chromium etchant, creatine kinase MM (CK-MM) fraction from human heart were from Sigma-Aldrich. CK peptide epitope was synthesized by Life Tein. The anti-CK-MM antibody (ab174635) was purchased from from Abcam. Sodium chloride (NaCl), dimethyl sulfoxide (DMSO) was from BDH. Gold-sputtered on glass (GoG) (5 nm Cr adhesion layer, 100 nm Au layer) was purchased from Deposition Research Lab, Inc (St. Charles, MO) with dimensions of 25.4 mm x 76.2 mm x 1.1 mm. AZ 40XT (positive photoresist) and AZ 300 MIF developer were obtained from Microchemicals. Polydimethylsiloxane (PDMS) was purchased from Dow Corning. Protein-oligo conjugation kit was obtained from Solulink, and 2kD molecular weight cut off (MWCO) Vivacon® 500 centrifugal concentrators from VWR. Custom, methylene blue-conjugated DNA (MB-DNA) was purchased from Biosearch Technologies (Novato, CA) and purified by RP-HPLC. Thiolated DNA was obtained from Integrated DNA Technologies (IDT; Coralville, Iowa), with purity confirmed by mass spectroscopy. T4 DNA ligase (400,000 units) and adenosine triphosphate (ATP, 10 mM) were from New England Biolabs. Prescreened human serum samples were acquired from BioIVT. Sequences of DNAs used in this work are listed in Table 1.0.

Experimental Methods

Preparation of Gold Electrodes. First, a photomask for the 2 mm diameter electrodes (18 identical electrodes on one mask) was designed in Adobe Illustrator, and the file was sent to Fineline Imaging (Colorado Springs, Colorado) for printing a positive photomask (see Figure S-1c). To achieve a photoresist pattern on GoG slides, a standard photolithographic procedure was used, followed by AZ photoresist and AZ developer. Then to remove excess gold and

chromium, GoG slides were introduced to gold etchant followed by chromium etchant for 30 s and 15 s, respectively. To remove remaining positive photoresist from the GoG slides, each slide was heated with DMSO at 150 °C for 30 min. Finally, electrodes were rinsed for 30 s with deionized water followed by ethanol and dried with nitrogen.

DNA monolayer assembly. Electrodes were cleaned with freshly prepared piranha solution prior to plasma oxidation. The piranha solution (H_2SO_4:H_2O_2, 3:1) was dropped on to the electrode surface and was washed away with deionized water after 1 min. Then, PDMS wells and gold electrodes were sonicated for 2 min in methanol and placed at 100 °C for 5 min. Next, both the electrodes and PDMS wells were plasma oxidized in an air plasma for 45 s (Harrick Plasma Cleaner). After permanently attaching the GoG slides and PDMS wells together, TCEP was used to reduce thio-DNA (5 µL of 10 µM thio-DNA with 5 µL of 3 mM TCEP) at room temperature for 1 hour. This mixture was diluted to a final concentration of 30 nM of thio-DNA using buffer (10 mM HEPES with 10 mM $MgCl_2$ at pH 7.0), then the diluted solution was added to the electrodes and incubated for 2 more hours. Next, 3 mM 6-mercaptohexanol (MCH) in buffer was dropped and incubated further for 1 hour. Lastly, to minimize protein adsorption onto PDMS or glass (surface passivation), the whole electrochemical cell was filled with 0.1 % BSA in buffer and was left for 30 min. After these steps, electrodes were ready to construct the nanostructure or could be stored up to a week at 4 °C.

Bioconjugation of creatine kinase peptide epitope and anchor-DNA. To conjugate creatine kinase peptide (CK peptide) with anchor DNA, both were separately activated with S-HyNic and S-4FB, respectively using the Protein-Oligo Conjugation Kits (Solulink), then aliquoted and stored at -20 °C (further details in Supporting Information). Next, when it was time to construct the nanostructure, both were mixed with recommended buffers and incubated at room temperature for 3 hours (**Figure 2**) to create DNA-epitope conjugates. These conjugates were subsequently used to construct the nanostructure, as described below.

DNA nanostructure construction by on-electrode enzymatic ligation. Once the electrodes included both thio-DNA and MCH self-assembled monolayers, they were ready for nanostructure assembly. A mixture containing 100 nM activated anchor DNA or amine-anchor DNA , 100 nM MB-DNA, 1.0 mM ATP, and 1.0 µL of 400,000 U T4 DNA ligase in buffer (0.5 $MgCl_2$, 0.1 % BSA, 10 mM HEPES, pH 7.0) was dropped onto the electrode surface, and this system was incubated at room temperature for 6 hours. Electrodes were then washed with deionized water for 30 s to remove excess reactants and unligated nanostructures. Finally, measuring buffer (0.5 NaCl, 0.1 % BSA, 10 mM HEPES) was introduced, and the measurement-ready nanostructure sensors were stored at 4 °C.

Electrochemical measurements. A Gamry reference 600 potentiostat was used for all EC measurements. To maintain precise temperatures during EC measurements, an in-house built Peltier system was used (**Figure S-3**). Temperature stability was also assisted by a mini-block heater (VWR) when measurement were not being made. When a sensor was ready for measurements, a silver/silver chloride (3 KCl) standard reference electrode (BASi) and platinum counter electrode (CH instruments) were introduced to a PDMS-defined well with a GoG electrode (custom electrochemical cell). Square-wave voltammograms (SVW) were measured from -0.450 to 0 V (versus reference) with a step size of 1 mV, a pulse height of 25 mV, and SWV frequencies from 100 to 900 Hz.

Anti-creatine kinase antibody detection. To obtain the calibration curve for anti-CK-MM antibody, solutions were added directly to the measurement-ready sensors. For steady-state measurements, first the SWV program was run in the measuring buffer (100 µL) to get a baseline, then this solution was removed and replaced with 100 µL of anti-CK-MM antibody solution (1 nM to 100 nM) and incubated at 37 °C for 30 min. The solution was removed again, and measuring buffer (100 µL) was introduced for the final SWV measurement. For kinetic measurements without CK-MM protein, after obtaining baseline measurement, 100 µL antibody in measuring buffer was added, and measurements were taken every 3 minutes for 1 hour.

Creatine kinase protein quantification. A competitive immunoassay protocol was followed to detect CK-MM protein. Once the nanostructure was ready, 50 nM of anti-CK-MM antibody was pre-incubated with various concentrations of CK-protein for 30 min at 37 °C. After obtaining the baseline measurement of each electrode in measuring buffer, the protein/antibody mixture was added onto the electrodes and incubated for another 30 min, followed by the addition of measuring buffer for final SWV measurements from 100 to 900 Hz. SWV data was processed with a linear baseline fit, and currents were reported as peak heights. The calibration curve was generated by averaging the peak responses at 500, 650, and 900 Hz with three different electrodes for each concentration.

Measurements in human serum. Small volumes of CK-MM protein and anti-CK-MM antibody were spiked into the serum samples to achieve 98% serum with the analyte present. For the buffer control sample, a small volume of antibody was spiked to achieve 99% of serum. Then the samples were incubated at 37 °C for 30 minutes. After the baseline measurement in measuring buffer, 40 µL of each mixture was incubated on the electrode for 1 hour. Finally, electrodes were washed with measuring buffer, and SWV measurements were done at 400 Hz in measuring buffer.

RESULTS AND DISCUSSION

Benefits of the DNA Nanostructure Sensor

In our recent work, we introduced the electrochemical DNA nanostructure for versatile detection of clinically relevant analytes[28, 29]. As it follows enzymatic ligation of three different short single stranded DNA on the electrode surface for immobilization, recognition and signaling, the nanostructure becomes a stable, single molecular unit on the electrode surface (**Figure 1**). The nanostructure is somewhat flexible and subjected to tethered diffusion and Brownian motion at the surface.[30], with a short oligonucleotide spacer to avoid detrimental double-layer effects on the double stranded DNA formation.[31] When a large enough target molecule is bound to the nanostructure, this movement slows, likely due to a combination of increased molecular weight and steric hindrance effects. Hence, diffusional

motion of methylene blue near the surface slows and provides an EC-based quantification method to analyze the target molecule's presence.

A key benefit of our DNA nanostructure architecture is that the central DNA strand (red strand in **Figure 1**), containing the binding unit, can be easily substituted without largely modifying the EC signaling mechanism. This is in contrast with aptasensors or E-AB sensors, which rely heavily on the binding-induced conformational changes of the aptamers and can exhibit much more variable EC responses with different targeted analytes. As shown in **Figure 1**, with our sensors, we first attach the thiol-DNA strand (blue) to the electrode surface, then we enzymatically ligate the binding strand (red) and signaling strand (brown) using T4 DNA ligase. Since the binding strand (red) can be easily substituted, the DNA nanostructure can be readily adapted to sense a wide variety of targets (**Figure 1, lower left**). We have thus far validated this concept with small molecule drugs (tacrolimus) and biotechnology controls (biotin, digoxigenin), a peptide drug (exendin-4), and larger antibodies (anti-digoxigenin, anti-tacrolimus, anti-exendin).[28, 29]

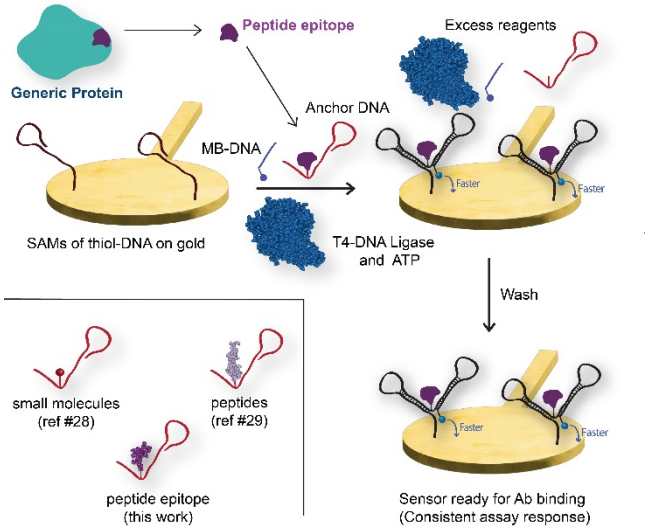

Figure 1. On-electrode assembly and ligation of the nanostructure. Peptide-epitope conjugation to the anchor DNA strand provides adaptability for sensing of a generic protein analyte, and on-electrode assembly permits simple washing of unlighted nanostructures, excess reagents, and other impurities. The final nanostructure is a single molecular unit with three covalent modifications (thiol-to-gold, peptide conjugate, and MB-DNA). *Bottom left panel:* Sensing via peptide epitopes (this work) expands the nanostructure sensors to detect generic proteins, a unique feature compared to prior work (refs 4 and 5).

Another benefit of this approach is cost savings. We have shown previously that the modular synthesis approach (three separate strands) for the surface-bound DNA nanostructure can provide very significant cost savings compared to commercial solid-phase synthesis of each customized structure (all three strands in one).[28] Lastly, because the final sensor consists of one single molecule of DNA with three synthetic modifications which is chemically attached to the gold electrode, the sensor can withstand various washing steps without significant loss of nanostructures. This issue permits simple washing of the DNA ligase and excess reagents from the surface after ligation, as shown in **Figure 1** (right).

Improving the sensor for generalized protein detection

However, as mentioned above, generalized protein sensing has not yet been accomplished with this architecture. While large antibodies can be easily detected, since they slow the tethered diffusion of the sensor significantly, and small molecules or peptides can be detected using indirect antibody displacement methods,[28, 29] most proteins of interest are too large to adapt to either of these methods. This issue was addressed in the current work by making DNA conjugates with the minimized antibody-binding epitope of the protein of interest. To validate the concept, we selected a larger protein as the analyte, creatine kinase (CK-MM; 86.2 kDa), an enzyme expressed in various cells and tissues that catalyzes the transformation of creatine to phosphocreatine with the help of ATP to provide energy to cells in need.[32] Levels of CK-MM in blood can elevate upon muscle damage, myocardial infarction, overexertion/rhabdomyolysis, or neuromuscular disorders,[33, 34] thus a rapid and direct EC sensor would be clinically advantageous. As shown in **Figure 2**, the antibody-binding peptide epitope (purple) of the CK-MM protein (cyan) was attached to the DNA nanostructure, which permitted quantitative biosensing of either the anti-CK antibody or the protein CK-MM.

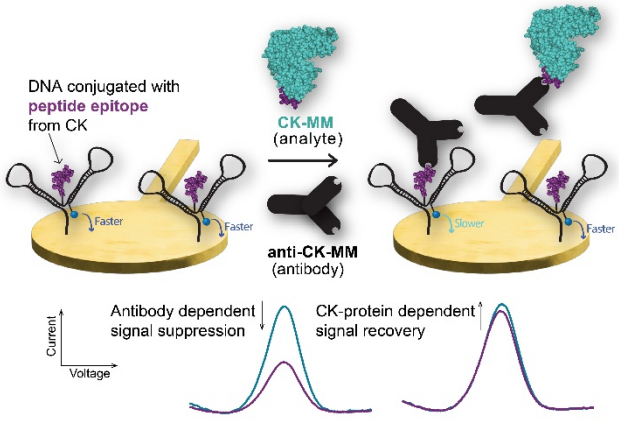

Figure 2. A more generalizable protein sensing approach was developed for the DNA nanostructure and applied to CK-MM sensing through a competitive immunoassay workflow.

Choice of peptide epitope and bioconjugation to DNA

Based on the commercial source of the antibody, the synthetic peptide sequence used as the immunogen to select the antibody is a 14 amino acid (14-aa; 1.7 kDa) segment of CK-MM (aa 5-18). We reasoned that this peptide was the ideal choice for antibody binding in our assay system, thus we used the sequence as part of the peptide epitope attached to the DNA nanostructure (purple segment in **Figure 2**). As in our recent work for exendin-4 sensing,[29] here we used a 2 kDa molecular weight cutoff column to purify the S-HyNic activated peptide (**Figure 3**, top left) during DNA-peptide conjugate synthesis. Since the 14-aa immunogen segment (1.7 kDa) was very close in size to the column's cutoff value, the peptide length was necessarily increased to

40-aa (Table S-2), giving a 4.4 kDa peptide that would be easily retained by the column. Originally, the intention was to use this larger 40-aa peptide (4.4 kDa) to simplify peptide activation with S-HyNic, then to cleave the peptide down to an 18-aa segment after bioconjugation was complete. For this reason, we incorporated a cleavage site of Factor Xa protease enzyme and an additional segment for solubility enhancement (QNG repeats).

The final conjugate, i.e. DNA coupled to the CK peptide epitope, is referred to herein as the "DNA-epitope conjugate." One way to confirm successful synthesis of the DNA-epitope conjugate via solution-phase conjugation is to compare the SWV current of the conjugates and the amine-tagged nanostructure (blank). Compared to the blank, there was a 40% decrease in SWV signal observed at 40 Hz, suggesting that the CK peptide epitope attachment to DNA caused a decreased tethered diffusion rate (**Figure 3**, right). To remove the excess amino acid linkage from the DNA-epitope conjugate, the system was incubated with factor Xa protease enzyme (in 100 mM NaCl, 10mM HEPES, and 0.1 % BSA) at room temperature for 3 hours, with the anticipation of an increase in signal during cleavage to a smaller, 18-aa segment of attached peptide. However, the current did not change during protease treatment. Without a significant difference in signals between enzyme-treated and untreated nanostructures, we decided to omit the factor Xa protease treatment and use the complete, DNA-epitope conjugate (with 40-aa peptide segment) for all remaining experiments in this study.

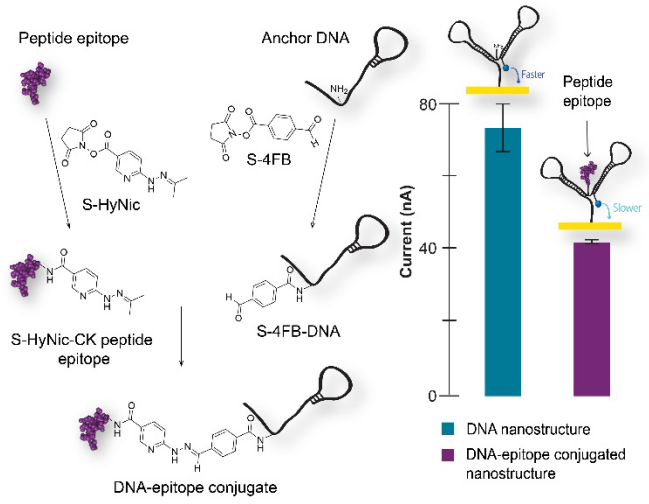

Figure 3. DNA-epitope conjugate synthesis through chemical activation of both the CK peptide epitope and anchor DNA. SWV current from nanostructures with unmodified anchor DNA (amine-tagged) (blue data) was compared to that of DNA-epitope modified nanostructures (purple), confirming bioconjugation. Error bars report standard deviations of triplicate electrode preparations.

EC Sensing of CK-MM antibody

Although this work was primarily designed for sensing CK-MM protein using an indirect approach (**Figure 2**), the first step was to confirm that anti-CK antibodies could be quantified with these electrodes. Thus, an additional application of these DNA nanostructures would be in generalizable, direct EC sensing of immune responses by detecting antibodies that bind various peptide segments. For example, virus or bacteria exposure, allergic reactions, or autoimmune reactions could be monitored rapidly and potentially at the POC with such sensors. To evaluate the system at this stage, varying antibody concentrations were added to the prepared nanostructures containing DNA-epitope conjugates. Antibodies caused a significant decrease in faradaic current using SWV readout. **Figure 4** shows the dynamic range of the antibody-responsive version of the nanostructure sensor to be from 0 – 50 nM, with a 3σ limit of detection (LOD) of 5 nM anti-CK-MM. Based on kinetic data (**Figure 5**, left) collected for 60 min after adding 70 nM of antibody (blue data), the sensor is capable of quantifying antibody in as little as 3 minutes, which bodes well for future POC applications in infectious disease or immune system monitoring. In fact, a similar concept could be used to detect any other antibody by conjugating its minimized peptide epitope sequence to the DNA nanostructure sensor.

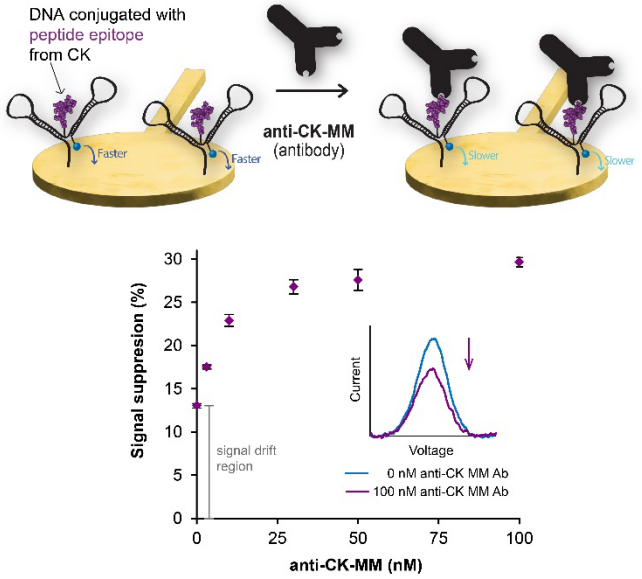

Figure 4. Antibody sensing mode. Direct detection of anti-CK-MM antibodies was first achieved with the nanostructure sensor. Calibration showed a dynamic range up to 100 nM and a 3σ LOD of 5 nM.

Potential Causes of Reduced Binding

Interestingly, this sensor's response to antibody addition was smaller than other antibody sensing responses in our previous reports,[28, 29] such that the 10-15% signal drifting effect in buffer became more prominent (**Figure 4**, shaded area). The signal drift in these and similar sensors is well known and can be accounted for in calibrations, and recent work has proven that electrochemical desorption of the monolayers on the electrode surface can be a major driving force for signal drift.[35] Since we carried out SWV at multiple frequencies and scanned from -0.450 to 0 V in all measurements, it is likely that EC desorption was a significant factor in our work as well.

With respect to the minimized response to antibody binding, it is possible that the peptide-oligo conjugate purity or stability are contributing factors. In our original work with these sensors,[28] streptavidin and anti-digoxigenin antibodies exhibited 70-80% signal suppression, and an antibody response from binding to a commercially synthesized DNA-

small molecule conjugate (DNA-tacrolimus) gave about 65% signal suppression. In follow-up work in sensing the peptide drug, exendin-4, we synthesized the DNA-peptide conjugates in house, and these sensors showed a lower response at 45% signal suppression.[29] Similarly, in this work, DNA-epitope conjugates were synthesized and purified in-house, and the antibody binding resulted in a maximum of about 32% signal suppression. Considering all this work, it is clear that peptide-oligo conjugates are more challenging to synthesize and purify compared to small-molecule conjugates. It is likely that improved responses could be achieved with more rigorous purification procedures such as liquid chromatography instead of using simpler MW cutoff columns. However, to minimize reaction scales with precious reagents in this proof-of-concept work for sensing generic proteins, use of chromatographic separation was considered out of the scope of the current work.

EC Sensing of CK-MM Protein

Although the antibody binding response was smaller than initially predicted, the sensor could still quickly quantify antibody binding in the nanomolar range. Thus, the next step was to evaluate the competitive immunoassay workflow (**Figure 2**) to permit sensing of the protein itself, CK-MM. For all these experiments, a known amount of anti-CK antibody (50 nM) was incubated with various concentrations of CK-MM at 37 °C for 30 minutes before adding to the sensor surface. To determine the fixed antibody concentration, the calibration curve in **Figure 4** and a real-time titration (Figure S-2) were used; the calibration saturated at about 50 nM antibody, and the titration showed a maximal response from 50 nM with diminished responses from higher concentrations (70 and 100 nM). Initial characterization of the sensor response kinetics (**Figure 5**, left) using 0 and 70 nM CK-MM showed that the protein could be distinguished from the blank within only 3 minutes, although waiting for 20-30 minutes provided larger signal differences. As in previous studies,[28, 29] this nanostructure sensor is thus capable of rapid sensing of the analyte, in this case being more generalizable to other proteins that were previously inaccessible to rapid EC sensing.

Calibration of the sensor against CK-MM protein was carried out using the competitive workflow and with 50 nM antibody. As shown in **Figure 5** (right), the sensor was evaluated in triplicate (3 electrodes each) by adding as much as 100 nM of CK-MM. The sensitivity was determined to be approximately 0.08 % nM^{-1}, and the 3σ LOD was determined to be 14 nM. The clinical range of CK-MM lies between 3 to 37 nM (shaded region in **Figure 5**), including male and female data,[36] overlapping with the sensor's dynamic range. While the sensor range should be extended to lower concentrations in the future to provide true clinical utility for healthy patients, conditions such as acute rhabdomyolysis due to crush injury often give CK-MM levels that exceed 200 times the upper reference limit.[37] Therefore, this sensor could be immediately useful for rhabdomyolysis monitoring, an application that would benefit from its rapid sensing capabilities.

Finally, the sensor was challenged in the presence of a complex sample matrix, 98% human serum. Because the measurement mechanism relies on antibody binding to a minimized peptide epitope that is covalently attached to DNA, it is important to confirm the binding will occur in the presence of clinically-relevant interfering components. Test serum samples were spiked with a mixture of 50 nM antibody and 70 nM CK-MM, while control serum samples were spiked with 50 nM antibody only. After electrode incubation for 1 hour to ensure signal stability, triplicate SWV measurements of these samples were compared to those in a background of only measurement buffer, and the data is shown in **Figure 6**. Comparing the differences in signal suppression between buffer and 98% serum matrices, the sensor in serum was able to recover 90% of the signal in buffer, boding well for future applications for fast, clinical CK-MM detection.

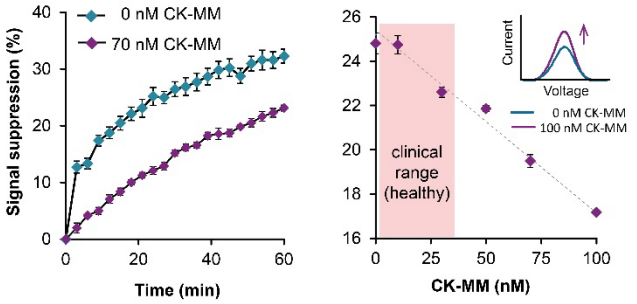

Figure 5. Protein sensing in the nM range with the DNA nanostructure. The kinetic study (SWV at 900 Hz) showed the ability to differentiate CK-MM protein within 3 minutes (left). The calibration (right) showed a linear dynamic range up to 100 nM CK-MM and an LOD of 14 nM, and this range overlapped with the normal human clinical range (healthy males and females) shown shaded in pink.

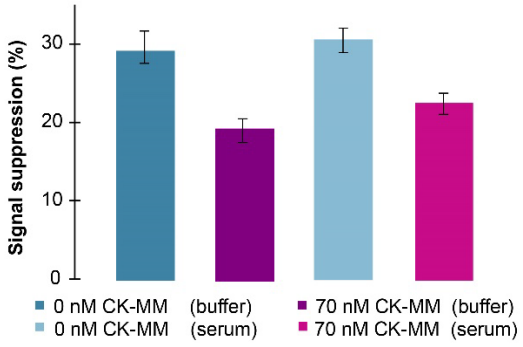

Figure 6. The sensor was functional in 98% human serum, with signals comparable to those in buffer (90% recovery).

Conclusion

In this work we have presented a new way to detect clinically relevant proteins by conjugating minimized antibody-binding peptide epitopes to our DNA nanostructure. Here, as a proof-of-concept of generalizable protein sensing, DNA-epitope conjugates were made for a sensor targeting CK-MM protein, which is a biomarker for clinical conditions—muscle damage, myocardial infarction, overexertion/rhabdomyolysis—that necessitate rapid measurement capabilities. The sensor was proven functional and capable of CK-MM measurements in only 3 minutes, and the dynamic

range overlapped with the human clinical range. While improvements in DNA-epitope conjugate purification is needed in the future, this work notably provides the first clear evidence that our nanostructure sensors can be adapted toward more generalizable protein sensing.

ASSOCIATED CONTENT

Supporting Information

The Supporting Information is available free of charge on the ACS Publications website.
List of DNA sequences used, information about amino acid sequence used, electrochemical cell fabrication, antibody calibration curve and temperature controlling system used.

AUTHOR INFORMATION

Corresponding Author

* Professor Christopher J. Easley - Department of Chemistry and Biochemistry, Auburn University, Auburn, Alabama 36849, United States; Orcid: https://orcid.org/0000-0002-2403-4147
;
Email: chris.easley@auburn.edu.

Author Contributions

A.G., S.S., N.K., and C.J.E. conceived the study, designed, and performed experiments, analyzed data, and collaboratively wrote the manuscript. A.S.N.K. performed experiments, analyzed data, and collaboratively wrote the manuscript. A.G., S.S., A.S.N.K., and N.K. performed experiments under the supervision of C.J.E.

Funding Sources

Research reported in this manuscript was supported by the National Institute of General Medical Sciences (NIGMS) of the National Institutes of Health (NIH) under award number R01 GM138828. The content of this manuscript is solely the responsibility of the authors and does not necessarily repre-sent the official views of the NIH.

Notes

The authors declare the following competing financial interest(s): The assay system reported in this manuscript has been patented under US patent 11,560,565 B2, and the authors have entered into a licensing agreement with an interested party.

REFERENCES

(1) Arroyo-Curras, N.; Somerson, J.; Vieira, P. A.; Ploense, K. L.; Kippin, T. E.; Plaxco, K. W. Real-time measurement of small molecules directly in awake, ambulatory animals. *Proc Natl Acad Sci U S A* **2017**, *114* (4), 645-650. DOI: 10.1073/pnas.1613458114.

(2) White, R. J.; Kallewaard, H. M.; Hsieh, W.; Patterson, A. S.; Kasehagen, J. B.; Cash, K. J.; Uzawa, T.; Soh, H. T.; Plaxco, K. W. Wash-free, electrochemical platform for the quantitative, multiplexed detection of specific antibodies. *Anal Chem* **2012**, *84* (2), 1098-1103. DOI: 10.1021/ac202757c.

(3) Rissin, D. M.; Kan, C. W.; Campbell, T. G.; Howes, S. C.; Fournier, D. R.; Song, L.; Piech, T.; Patel, P. P.; Chang, L.; Rivnak, A. J.; et al. Single-molecule enzyme-linked immunosorbent assay detects serum proteins at subfemtomolar concentrations. *Nat Biotechnol* **2010**, *28* (6), 595-599. DOI: 10.1038/nbt.1641.

(4) Parolo, C.; Idili, A.; Ortega, G.; Csordas, A.; Hsu, A.; Arroyo-Curras, N.; Yang, Q.; Ferguson, B. S.; Wang, J.; Plaxco, K. W. Real-Time Monitoring of a Protein Biomarker. *ACS Sens* **2020**, *5* (7), 1877-1881. DOI: 10.1021/acssensors.0c01085.

(5) Ullman, E. F.; Kirakossian, H.; Singh, S.; Wu, Z. P.; Irvin, B. R.; Pease, J. S.; Switchenko, A. C.; Irvine, J. D.; Dafforn, A.; Skold, C. N. Luminescent oxygen channeling immunoassay: measurement of particle binding kinetics by chemiluminescence. *Proc Natl Acad Sci U S A* **1994**, *91* (12), 5426-5430.

(6) Beaudet, L.; Rodriguez-Suarez, R.; Venne, M.-H.; Caron, M.; Bédard, J.; Brechler, V.; Parent, S.; Bielefeld-Sévigny, M. AlphaLISA immunoassays: the no-wash alternative to ELISAs for research and drug discovery. *Nature Methods* **2008**, *5* (12), an8-an9. DOI: 10.1038/nmeth.f.230.

(7) Arts, R.; den Hartog, I.; Zijlema, S. E.; Thijssen, V.; van der Beelen, S. H. E.; Merkx, M. Detection of Antibodies in Blood Plasma Using Bioluminescent Sensor Proteins and a Smartphone. *Anal Chem* **2016**, *88* (8), 4525-4532. DOI: 10.1021/acs.analchem.6b00534.

(8) Huang, L.; Chen, J.; Yu, Z.; Tang, D. Self-Powered Temperature Sensor with Seebeck Effect Transduction for Photothermal–Thermoelectric Coupled Immunoassay. *Anal Chem* **2020**, *92* (3), 2809-2814. DOI: 10.1021/acs.analchem.9b05218.

(9) Zhang, B.; Hu, X.; Jia, Y.; Li, J.; Zhao, Z. Polyaniline@Au organic-inorganic nanohybrids with thermometer readout for photothermal immunoassay of tumor marker. *Microchimica Acta* **2021**, *188* (3), 63. DOI: 10.1007/s00604-021-04719-y.

(10) Shi, N.; Easley, C. J. Programmable μChopper Device with On-Chip Droplet Mergers for Continuous Assay Calibration. *Micromachines* **2020**, *11* (6), 620.

(11) Clifford, A.; Das, J.; Yousefi, H.; Mahmud, A.; Chen, J. B.; Kelley, S. O. Strategies for Biomolecular Analysis and Continuous Physiological Monitoring. *J Am Chem Soc* **2021**, *143* (14), 5281-5294. DOI: 10.1021/jacs.0c13138.

(12) Di Nardo, F.; Chiarello, M.; Cavalera, S.; Baggiani, C.; Anfossi, L. Ten Years of Lateral Flow Immunoassay Technique Applications: Trends, Challenges and Future Perspectives. *Sensors* **2021**, *21* (15), 5185.

(13) Cash, K. J.; Ricci, F.; Plaxco, K. W. An electrochemical sensor for the detection of protein-small molecule interactions directly in serum and other complex matrices. *J Am Chem Soc* **2009**, *131* (20), 6955-6957. DOI: 10.1021/ja9011595.

(14) Ou, D.; Sun, D.; Lin, X.; Liang, Z.; Zhong, Y.; Chen, Z. A dual-aptamer-based biosensor for specific detection of breast cancer biomarker HER2 via flower-like nanozymes and DNA nanostructures. *J Mater Chem B* **2019**, *7* (23), 3661-3669. DOI: 10.1039/c9tb00472f.

(15) Leonard, E. K.; Aller Pellitero, M.; Juelg, B.; Spangler, J. B.; Arroyo-Currás, N. Antibody–Invertase Fusion Protein Enables Quantitative Detection of SARS-CoV-2 Antibodies Using Widely Available Glucometers. *J Am Chem Soc* **2022**, *144* (25), 11226-11237. DOI: 10.1021/jacs.2c02537.

(16) Li, H.; Dauphin-Ducharme, P.; Ortega, G.; Plaxco, K. W. Calibration-Free Electrochemical Biosensors Supporting Accurate Molecular Measurements Directly in Undiluted Whole Blood. *J Am Chem Soc* **2017**, *139* (32), 11207-11213. DOI: 10.1021/jacs.7b05412.

(17) Ogden, N. E.; Kurnik, M.; Parolo, C.; Plaxco, K. W. An electrochemical scaffold sensor for rapid syphilis diagnosis. *Analyst* **2019**, *144* (17), 5277-5283. DOI: 10.1039/c9an00455f.

(18) Das, J.; Gomis, S.; Chen, J. B.; Yousefi, H.; Ahmed, S.; Mahmud, A.; Zhou, W.; Sargent, E. H.; Kelley, S. O. Reagentless biomolecular analysis using a molecular pendulum. *Nature Chem* **2021**, *13* (5), 428-434. DOI: 10.1038/s41557-021-00644-y.

(19) Arroyo-Currás, N.; Dauphin-Ducharme, P.; Scida, K.; Chávez, J. L. From the beaker to the body: translational challenges for

electrochemical, aptamer-based sensors. *Anal Methods* **2020**, *12* (10), 1288-1310. DOI: 10.1039/d0ay00026d.

(20) Mahshid, S. S.; Ricci, F.; Kelley, S. O.; Vallee-Belisle, A. Electrochemical DNA-Based Immunoassay That Employs Steric Hindrance To Detect Small Molecules Directly in Whole Blood. *ACS Sens* **2017**, *2* (6), 718-723. DOI: 10.1021/acssensors.7b00176.

(21) Soria-Guerra, R. E.; Nieto-Gomez, R.; Govea-Alonso, D. O.; Rosales-Mendoza, S. An overview of bioinformatics tools for epitope prediction: Implications on vaccine development. *J Biomed Inform* **2015**, *53*, 405-414. DOI: https://doi.org/10.1016/j.jbi.2014.11.003.

(22) Palladino, P.; Minunni, M.; Scarano, S. Cardiac Troponin T capture and detection in real-time via epitope-imprinted polymer and optical biosensing. *Biosens Bioelectron* **2018**, *106*, 93-98. DOI: https://doi.org/10.1016/j.bios.2018.01.068.

(23) Mahshid, S. S.; Mahshid, S.; Vallee-Belisle, A.; Kelley, S. O. Peptide-Mediated Electrochemical Steric Hindrance Assay for One-Step Detection of HIV Antibodies. *Anal Chem* **2019**, *91* (8), 4943-4947. DOI: 10.1021/acs.analchem.9b00648.

(24) Gerasimov, J. Y.; Lai, R. Y. An electrochemical peptide-based biosensing platform for HIV detection. *Chem Commun* **2010**, *46* (3), 395-397. DOI: 10.1039/b919070h.

(25) Langer, A.; Hampel, P. A.; Kaiser, W.; Knezevic, J.; Welte, T.; Villa, V.; Maruyama, M.; Svejda, M.; Jähner, S.; Fischer, F.; et al. Protein analysis by time-resolved measurements with an electro-switchable DNA chip. *Nat Commun* **2013**, *4* (1), 2099. DOI: 10.1038/ncomms3099.

(26) Kroener, F.; Heerwig, A.; Kaiser, W.; Mertig, M.; Rant, U. Electrical Actuation of a DNA Origami Nanolever on an Electrode. *J Am Chem Soc* **2017**, *139* (46), 16510-16513. DOI: 10.1021/jacs.7b10862.

(27) Kang, D.; Parolo, C.; Sun, S.; Ogden, N. E.; Dahlquist, F. W.; Plaxco, K. W. Expanding the Scope of Protein-Detecting Electrochemical DNA "Scaffold" Sensors. *ACS Sens* **2018**, *3* (7), 1271-1275. DOI: 10.1021/acssensors.8b00311.

(28) Somasundaram, S.; Easley, C. J. A Nucleic Acid Nanostructure Built through On-Electrode Ligation for Electrochemical Detection of a Broad Range of Analytes. *J Am Chem Soc* **2019**, *141* (29), 11721-11726. DOI: 10.1021/jacs.9b06229.

(29) Khuda, N.; Somasundaram, S.; Easley, C. J. Electrochemical Sensing of the Peptide Drug Exendin-4 Using a Versatile Nucleic Acid Nanostructure. *ACS Sens* **2022**, *7* (3), 784-789. DOI: 10.1021/acssensors.1c02336.

(30) Huang, K. C.; White, R. J. Random walk on a leash: a simple single-molecule diffusion model for surface-tethered redox molecules with flexible linkers. *J Am Chem Soc* **2013**, *135* (34), 12808-12817. DOI: 10.1021/ja4060788.

(31) Khuda, N.; Somasundaram, S.; Urgunde, A. B.; Easley, C. J. Ionic Strength and Hybridization Position near Gold Electrodes Can Significantly Improve Kinetics in DNA-Based Electrochemical Sensors. *ACS Appl Mater Interfaces* **2023**, *15* (4), 5019-5027. DOI: 10.1021/acsami.2c22741.

(32) Baird, M. F.; Graham, S. M.; Baker, J. S.; Bickerstaff, G. F. Creatine-kinase- and exercise-related muscle damage implications for muscle performance and recovery. *J Nutr Metab* **2012**, *2012*, 960363. DOI: 10.1155/2012/960363 From NLM.

(33) McLeish, M. J.; Kenyon, G. L. Relating structure to mechanism in creatine kinase. *Crit Rev Biochem Mol Biol* **2005**, *40* (1), 1-20. DOI: 10.1080/10409230590918577.

(34) Morandi, L.; Angelini, C.; Prelle, A.; Pini, A.; Grassi, B.; Bernardi, G.; Politano, L.; Bruno, C.; De Grandis, D.; Cudia, P.; et al. High plasma creatine kinase: review of the literature and proposal for a diagnostic algorithm. *Neurol Sci* **2006**, *27* (5), 303-311. DOI: 10.1007/s10072-006-0701-0.

(35) Leung, K. K.; Downs, A. M.; Ortega, G.; Kurnik, M.; Plaxco, K. W. Elucidating the Mechanisms Underlying the Signal Drift of Electrochemical Aptamer-Based Sensors in Whole Blood. *ACS Sens* **2021**, *6* (9), 3340-3347. DOI: 10.1021/acssensors.1c01183.

(36) *Creatine Kinase (CK), Serum - Clinical & Interpretive*. Mayo Foundation for Medical Education and Research, 2023. https://www.mayocliniclabs.com/test-catalog/Overview/8336#Clinical-and-Interpretive (accessed 2023 January 27).

(37) Burtis, C. A. R., N.; Bruns, D. E. *Tietz Fundamentals of Clinical Chemistry and Molecular Diagnostics - eBook*; Elsevier, 2015.

Insert Table of Contents artwork here

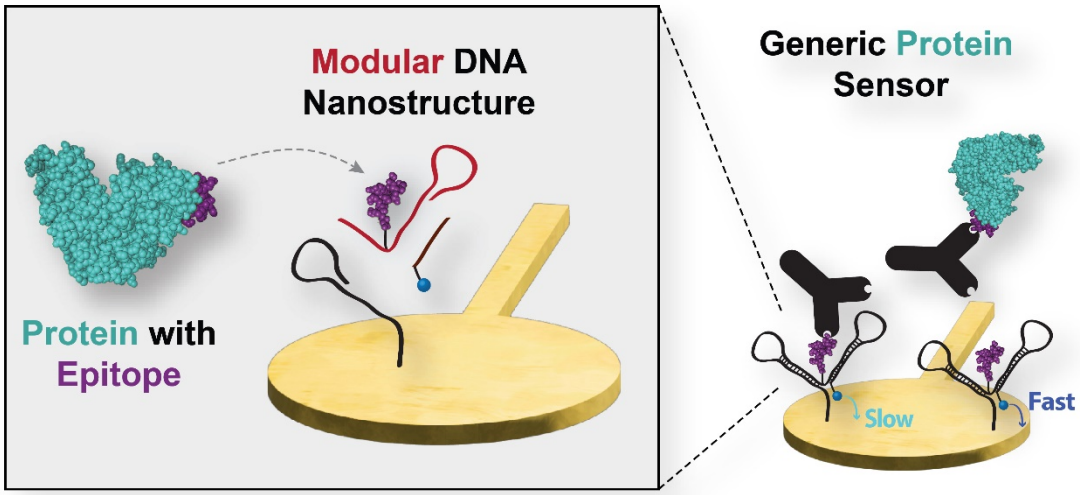
Modular DNA
Nanostructure
Protein with
Epitope
Generic Protein
Sensor
Slow
Fast